

## Supplementary Material for

### **Quantum entanglement of the spin and orbital angular momentum of photons using metamaterials**

Tomer Stav, Arkady Faerman, Elhanan Maguid, Dikla Oren, Vladimir Kleiner,  
Erez Hasman\*, Mordechai Segev\*

\*Corresponding author. Email: [mehasman@technion.ac.il](mailto:mehasman@technion.ac.il) (E.H.); [msegev@technion.ac.il](mailto:msegev@technion.ac.il) (M.S.)

Published 14 September 2018, *Science* **361**, 1101 (2017)  
DOI: 10.1126/science.aat9042

#### This PDF file includes:

- Materials and Methods
- Supplementary Text
- Fig. S1
- Table S1
- References

## Materials and Methods

### Fabrication of Si-GPM

The poly-Si thin film with a thickness of 300nm was grown at a temperature of 590°C on a SiO<sub>2</sub> (fused silica) substrate. The photoresist CSAR 6200.09 (Allresist GmbH, Germany) with a thickness of 190nm was deposited on the poly-Si film and baked at 150°C for 1 minute. For transferring the pattern onto the poly-Si film, the photoresist mask was made using Raith EBPG5200 E-beam lithography system (Raith, Germany), then baked at 130°C for 1 minute, and subsequently etched using deep reactive-ion etching by F-ICP Plasma Therm system (Plasma-Therm, FL, USA) for 30 seconds..

### Supplementary Text

#### Quantum state tomography and reconstruction of the density matrix

To verify that the state emerging from the metasurface is indeed entangled, for example the Bell state:

$$|\Phi^+\rangle = \frac{1}{\sqrt{2}}(|\sigma_+\rangle|\ell=1\rangle + |\sigma_-\rangle|\ell=-1\rangle),$$

the density matrix must be recovered. Theoretically, the density matrix for this state is by definition:

$$\rho = |\Phi^+\rangle\langle\Phi^+| = \left( \frac{|\sigma_+\rangle|\ell=1\rangle + |\sigma_-\rangle|\ell=-1\rangle}{\sqrt{2}} \right) \left( \frac{\langle\sigma_+|\langle\ell=1| + \langle\sigma_-|\langle\ell=-1|}{\sqrt{2}} \right).$$

To perform the measurements, we shall pass the photon exiting the GPM through a SLM that projects the wavefunction onto the different elements of the OAM basis. Subsequently, we convert only the conjugated states back to  $|\ell=0\rangle$ , and couple them into the fiber of the SPCM. For spin basis projection, these states are passed through a QWP, HWP and Pol.

To perform QST, a tomographically complete set of measurements is required. We show that to fulfill this requirement for the OAM qubit, we chose the following measurements:

$$\begin{aligned} \hat{v}_1 &= |\ell=1\rangle\langle\ell=1| \\ \hat{v}_2 &= |\ell=-1\rangle\langle\ell=-1| \\ \hat{v}_3 &= |+\rangle\langle+| = \frac{1}{\sqrt{2}}(|\ell=1\rangle + |\ell=-1\rangle) \frac{1}{\sqrt{2}}(|\ell=1\rangle + |\ell=-1\rangle)^\dagger \\ \hat{v}_4 &= |r\rangle\langle r| = \frac{1}{\sqrt{2}}(|\ell=1\rangle - i|\ell=-1\rangle) \frac{1}{\sqrt{2}}(|\ell=1\rangle - i|\ell=-1\rangle)^\dagger \end{aligned}$$

and for the spin qubit we chose:

$$\begin{aligned}
\hat{\mu}_1 &= |H\rangle\langle H| \\
\hat{\mu}_2 &= |V\rangle\langle V| \\
\hat{\mu}_3 &= |D\rangle\langle D| = \frac{1}{\sqrt{2}}(|H\rangle + |V\rangle) \frac{1}{\sqrt{2}}(|H\rangle + |V\rangle)^\dagger \\
\hat{\mu}_4 &= |\sigma_+\rangle\langle\sigma_+| = \frac{1}{\sqrt{2}}(|H\rangle - i|V\rangle) \frac{1}{\sqrt{2}}(|H\rangle - i|V\rangle)^\dagger
\end{aligned}$$

If we find a set of  $4 \times 4$  matrices  $\hat{\Gamma}$  that satisfy  $\text{Tr}[\hat{\Gamma}_\alpha \hat{\Gamma}_\beta] = \delta_{\alpha\beta}$ , where  $\alpha, \beta = 1, 2, \dots, 16$ , the set of measurements  $\hat{P}_{ij} = \hat{\mu}_i \otimes \hat{\nu}_j$  is tomographically complete, if and only if, the matrix  $B_{\beta\alpha} = \text{Tr}[\hat{\Gamma}_\alpha \hat{P}_\beta]$  is non-singular.

The matrix  $B$  is calculated according to the set of  $\hat{P}_{ij}$  measurements described in Table 1 and the  $\hat{\Gamma}$  matrices that are simply  $SU(2) \otimes SU(2)$  generators. For the chosen  $\hat{\Gamma}$ , we find that  $|B| = -0.0039$  and therefore non-singular, which means that the set is tomographically complete.

In order to reconstruct the density matrix from these measurements, we define

$$n_{ij} = \mathcal{N} \text{Tr}[\hat{\rho} \hat{P}_{ij}].$$

We can find the normalization factor  $\mathcal{N}$  easily by making the first measurement without any projections (intensity) and get  $n_0 = \mathcal{N} \text{Tr}[\hat{\rho} \mathbb{I}] = \mathcal{N}$ .

The normalized measurements are defined as

$$s_{ij} = \frac{n_{ij}}{n_0} = \text{Tr}[\hat{\rho} \hat{P}_{ij}].$$

One can reconstruct the density matrix simply by

$$\hat{\rho} = \sum_{\alpha=1}^{16} \sum_{\beta=1}^{16} s_\alpha (B^{-1})_{\alpha\beta} \hat{\Gamma}_\beta \quad (1).$$

However, calculating  $\hat{\rho}$  this way is not optimal, due to the experimental errors in the measured  $s_\alpha$  vector. Simply taking the inverse of the matrix  $B$  and substituting it in  $s_\alpha$  in Eq. 1 does not take into account the fact that  $\hat{\rho}$  should be a physical density matrix that contains variances in the experimental measurements. Therefore, we use a Maximum Likelihood Estimation (MLE) approach. Under the assumption of Gaussian noise, MLE is equivalent to least squares (34). Since  $\hat{\Gamma}_\alpha$  constitute an orthonormal set, we can write the density matrix as

$$\hat{\rho} = \sum_{\alpha=1}^{16} r_\alpha \hat{\Gamma}_\alpha \quad (2).$$

From Eqs. 1 and 2 we see that  $\vec{s} = B\vec{r}$  and we can find the vector  $\vec{r}$  by least squares with the proper constraints:

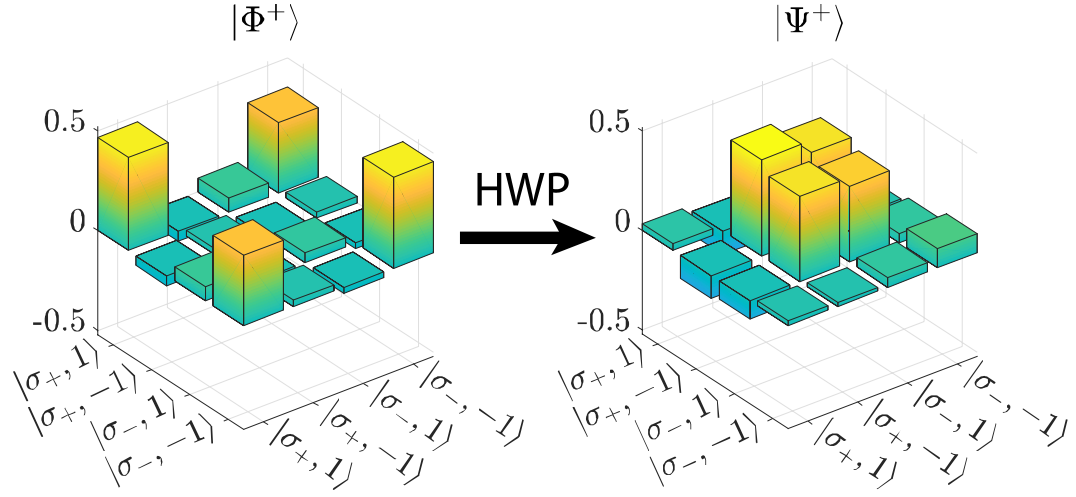
$$\begin{aligned}
&\text{minimize } \|\vec{s} - B\vec{r}\|_2 \\
&\text{such that } \hat{\rho} = \hat{\rho}^\dagger \\
&\quad \hat{\rho} \geq 0 \\
&\quad \text{Tr } \hat{\rho} = 1
\end{aligned}$$

We use the order described in Table 1 to take these measurements.

## Single particle entanglement for quantum information

The main text presents entangled states generated both on a single photon (Figs. 1-3) and on biphoton states (Fig. 4). In all cases the entanglement is generated by the metasurface (the GPM in Figs. 2 and 4). Entanglement on biphoton states is widely considered as the building block of optical quantum information systems, but entanglement on single photon states has been argued to be “classical entanglement” (37). However, as shown by (37), this type of entanglement on a single particle holds quantum properties which cannot be reproduced with classical light, and hence can be used in quantum computation and other quantum information schemes. Several schemes have been proposed for the utilization of two qubits encoded on a single photon for quantum information processing. In fact, several quantum gates (including universal quantum gates) and quantum algorithms based on entanglement on a single particle have been proposed (38). Experimentally, a quantum controlled-NOT gate based on entangled states on single photon has been demonstrated in the lab (39). One should not confuse a non-separable classical mode (which features classical entanglement) with an entangled state of a single photon. For example, generation of a non-separable classical mode was demonstrated using classical light (39) (manifesting “classical entanglement”). However, even in that experiment (39), when a single photon was passed through the same apparatus - it generated a genuinely entangled quantum state.

**Fig. S1.**

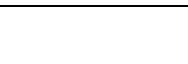


**Fig. S1. SWAP gate following the metasurface.**

The measured density matrix of the state  $|\Phi^+\rangle$ , which is generated by the GPM. After passing through a HWP the state is transformed into  $|\Psi^+\rangle$ , by performing a SWAP gate on the spin qubit, leaving the OAM qubit unaffected. The experimental density matrix coincides with the theoretical results at fidelity higher than 90%.

**Table S1.**

List of measurements of the QST. The SLM phase profile range are from 0 (black) to  $2\pi$  (white).

Order	Projection	QWP [deg]	HWP [deg]	SLM profile
0	Intensity	-	-	-
1	$ H\rangle \ell = 1\rangle$	0	0	
2	$ V\rangle \ell = 1\rangle$	0	45	
3	$ \sigma_+\rangle \ell = 1\rangle$	0	22.5	
4	$ D\rangle \ell = 1\rangle$	45	22.5	
5	$ D\rangle \ell = -1\rangle$	45	22.5	
6	$ \sigma_+\rangle \ell = -1\rangle$	0	22.5	
7	$ V\rangle \ell = -1\rangle$	0	45	
8	$ H\rangle \ell = -1\rangle$	0	0	
9	$ H\rangle +\rangle$	0	0	
10	$ V\rangle +\rangle$	0	45	
11	$ \sigma_+\rangle +\rangle$	0	22.5	
12	$ D\rangle +\rangle$	45	22.5	
13	$ D\rangle r\rangle$	45	22.5	
14	$ \sigma_+\rangle r\rangle$	0	22.5	
15	$ V\rangle r\rangle$	0	45	
16	$ H\rangle r\rangle$	0	0	

## References and Notes

1. J. B. Pendry, Negative refraction makes a perfect lens. *Phys. Rev. Lett.* **85**, 3966–3969 (2000). [doi:10.1103/PhysRevLett.85.3966](https://doi.org/10.1103/PhysRevLett.85.3966) Medline
2. V. M. Shalaev, Optical negative-index metamaterials. *Nat. Photonics* **1**, 41–48 (2007). [doi:10.1038/nphoton.2006.49](https://doi.org/10.1038/nphoton.2006.49)
3. D. Schurig, J. J. Mock, B. J. Justice, S. A. Cummer, J. B. Pendry, A. F. Starr, D. R. Smith, Metamaterial electromagnetic cloak at microwave frequencies. *Science* **314**, 977–980 (2006). [doi:10.1126/science.1133628](https://doi.org/10.1126/science.1133628) Medline
4. M. Silveirinha, N. Engheta, Tunneling of electromagnetic energy through subwavelength channels and bends using  $\epsilon$ -near-zero materials. *Phys. Rev. Lett.* **97**, 157403 (2006). [doi:10.1103/PhysRevLett.97.157403](https://doi.org/10.1103/PhysRevLett.97.157403) Medline
5. I. Liberal, N. Engheta, Near-zero refractive index photonics. *Nat. Photonics* **11**, 149–158 (2017). [doi:10.1038/nphoton.2017.13](https://doi.org/10.1038/nphoton.2017.13)
6. Z. Bomzon, V. Kleiner, E. Hasman, Pancharatnam—Berry phase in space-variant polarization-state manipulations with subwavelength gratings. *Opt. Lett.* **26**, 1424–1426 (2001). [doi:10.1364/OL.26.001424](https://doi.org/10.1364/OL.26.001424) Medline
7. Z. Bomzon, G. Biener, V. Kleiner, E. Hasman, Space-variant Pancharatnam-Berry phase optical elements with computer-generated subwavelength gratings. *Opt. Lett.* **27**, 1141–1143 (2002). [doi:10.1364/OL.27.001141](https://doi.org/10.1364/OL.27.001141) Medline
8. A. V. Kildishev, A. Boltasseva, V. M. Shalaev, Planar photonics with metasurfaces. *Science* **339**, 1232009 (2013). [doi:10.1126/science.1232009](https://doi.org/10.1126/science.1232009) Medline
9. A. Pors, O. Albrektsen, I. P. Radko, S. I. Bozhevolnyi, Gap plasmon-based metasurfaces for total control of reflected light. *Sci. Rep.* **3**, 2155 (2013). [doi:10.1038/srep02155](https://doi.org/10.1038/srep02155) Medline
10. X. Yin, Z. Ye, J. Rho, Y. Wang, X. Zhang, Photonic spin Hall effect at metasurfaces. *Science* **339**, 1405–1407 (2013). [doi:10.1126/science.1231758](https://doi.org/10.1126/science.1231758) Medline
11. N. Yu, P. Genevet, M. A. Kats, F. Aieta, J.-P. Tetienne, F. Capasso, Z. Gaburro, *Science* **334**, 333–337 (2011). [doi:10.1126/science.1231758](https://doi.org/10.1126/science.1231758)
12. D. Lin, P. Fan, E. Hasman, M. L. Brongersma, Dielectric gradient metasurface optical elements. *Science* **345**, 298–302 (2014). [doi:10.1126/science.1253213](https://doi.org/10.1126/science.1253213) Medline
13. K. E. Chong, I. Staude, A. James, J. Dominguez, S. Liu, S. Campione, G. S. Subramania, T. S. Luk, M. Decker, D. N. Neshev, I. Brener, Y. S. Kivshar, Polarization-independent silicon metadevices for efficient optical wavefront control. *Nano Lett.* **15**, 5369–5374 (2015). [doi:10.1021/acs.nanolett.5b01752](https://doi.org/10.1021/acs.nanolett.5b01752) Medline
14. A. Arbabi, Y. Horie, M. Bagheri, A. Faraon, Dielectric metasurfaces for complete control of phase and polarization with subwavelength spatial resolution and high transmission. *Nat. Nanotechnol.* **10**, 937–943 (2015). [doi:10.1038/nnano.2015.186](https://doi.org/10.1038/nnano.2015.186) Medline
15. A. I. Kuznetsov, A. E. Miroshnichenko, M. L. Brongersma, Y. S. Kivshar, B. Luk'yanchuk, Optically resonant dielectric nanostructures. *Science* **354**, aag2472 (2016). [doi:10.1126/science.aag2472](https://doi.org/10.1126/science.aag2472) Medline

16. T. Roger, S. Vezzoli, E. Bolduc, J. Valente, J. J. F. Heitz, J. Jeffers, C. Soci, J. Leach, C. Couteau, N. I. Zheludev, D. Faccio, Coherent perfect absorption in deeply subwavelength films in the single-photon regime. *Nat. Commun.* **6**, 7031 (2015). [doi:10.1038/ncomms8031](https://doi.org/10.1038/ncomms8031) [Medline](#)
17. M. Siomau, A. A. Kamli, A. A. Moiseev, B. C. Sanders, Entanglement creation with negative index metamaterials. *Phys. Rev. A* **85**, 050303 (2012). [doi:10.1103/PhysRevA.85.050303](https://doi.org/10.1103/PhysRevA.85.050303)
18. L. K. Grover, A fast quantum mechanical algorithm for database search. *Proc. twenty-eighth Annu. ACM Symp. Theory Comput. ACM*, 212–219 (1996).
19. P. W. Shor, Algorithms for quantum computation: discrete logarithms and factoring. *Proc. 35th Annu. Symp. Found. Comput. Sci. IEEE*, 124–134 (1994).
20. D. Deutsch, R. Jozsa, Rapid solution of problems by quantum computation. *Proc. R. Soc. Lond. A* **439**, 553–558 (1992). [doi:10.1098/rspa.1992.0167](https://doi.org/10.1098/rspa.1992.0167)
21. B. G. Englert, C. Kurtsiefer, H. Weinfurter, Universal unitary gate for single-photon two-qubit states. *Phys. Rev. A* **63**, 032303 (2001). [doi:10.1103/PhysRevA.63.032303](https://doi.org/10.1103/PhysRevA.63.032303)
22. A. Mair, A. Vaziri, G. Weihs, A. Zeilinger, Entanglement of the orbital angular momentum states of photons. *Nature* **412**, 313–316 (2001). [doi:10.1038/35085529](https://doi.org/10.1038/35085529) [Medline](#)
23. J. Leach, B. Jack, J. Romero, A. K. Jha, A. M. Yao, S. Franke-Arnold, D. G. Ireland, R. W. Boyd, S. M. Barnett, M. J. Padgett, Quantum correlations in optical angle-orbital angular momentum variables. *Science* **329**, 662–665 (2010). [doi:10.1126/science.1190523](https://doi.org/10.1126/science.1190523) [Medline](#)
24. L. Shi, E. J. Galvez, R. R. Alfano, Photon entanglement through brain tissue. *Sci. Rep.* **6**, 37714 (2016). [doi:10.1038/srep37714](https://doi.org/10.1038/srep37714) [Medline](#)
25. J. W. Silverstone, D. Bonneau, K. Ohira, N. Suzuki, H. Yoshida, N. Iizuka, M. Ezaki, C. M. Natarajan, M. G. Tanner, R. H. Hadfield, V. Zwiller, G. D. Marshall, J. G. Rarity, J. L. O’Brien, M. G. Thompson, On-chip quantum interference between silicon photon-pair sources. *Nat. Photonics* **8**, 104–108 (2014). [doi:10.1038/nphoton.2013.339](https://doi.org/10.1038/nphoton.2013.339)
26. M. Kues, C. Reimer, P. Roztocki, L. R. Cortés, S. Sciara, B. Wetzel, Y. Zhang, A. Cino, S. T. Chu, B. E. Little, D. J. Moss, L. Caspani, J. Azaña, R. Morandotti, On-chip generation of high-dimensional entangled quantum states and their coherent control. *Nature* **546**, 622–626 (2017). [doi:10.1038/nature22986](https://doi.org/10.1038/nature22986) [Medline](#)
27. E. Altewischer, M. P. van Exter, J. P. Woerdman, Plasmon-assisted transmission of entangled photons. *Nature* **418**, 304–306 (2002). [doi:10.1038/nature00869](https://doi.org/10.1038/nature00869) [Medline](#)
28. M. S. Tame, K. R. McEnergy, Ş. K. Özdemir, J. Lee, S. A. Maier, M. S. Kim, Quantum plasmonics. *Nat. Phys.* **9**, 329–340 (2013). [doi:10.1038/nphys2615](https://doi.org/10.1038/nphys2615)
29. E. Maguid, I. Yulevich, M. Yannai, V. Kleiner, M. L Brongersma, E. Hasman, Multifunctional interleaved geometric-phase dielectric metasurfaces. *Light Sci. Appl.* **6**, e17027 (2017). [doi:10.1038/lsa.2017.27](https://doi.org/10.1038/lsa.2017.27)
30. M. V. Berry, Quantal phase factors accompanying adiabatic changes. *Proc. R. Soc. London Ser. A* **392**, 45–57 (1984). [doi:10.1098/rspa.1984.0023](https://doi.org/10.1098/rspa.1984.0023)

31. K. Y. Bliokh, F. J. Rodríguez-Fortuño, F. Nori, A. V. Zayats, Spin–orbit interactions of light. *Nat. Photonics* **9**, 796–808 (2015). [doi:10.1038/nphoton.2015.201](https://doi.org/10.1038/nphoton.2015.201)
32. K. Y. Bliokh, F. Nori, Transverse and longitudinal angular momenta of light. *Phys. Rep.* **592**, 1–38 (2015). [doi:10.1016/j.physrep.2015.06.003](https://doi.org/10.1016/j.physrep.2015.06.003)
33. E. Nagali, F. Sciarrino, F. De Martini, L. Marrucci, B. Piccirillo, E. Karimi, E. Santamato, Quantum information transfer from spin to orbital angular momentum of photons. *Phys. Rev. Lett.* **103**, 013601 (2009). [doi:10.1103/PhysRevLett.103.013601](https://doi.org/10.1103/PhysRevLett.103.013601) Medline
34. Materials and methods are available as supplementary materials.
35. D. F. V. James, P. G. Kwiat, W. J. Munro, A. G. White, Measurement of qubits. *Phys. Rev. A* **64**, 052312 (2001). [doi:10.1103/PhysRevA.64.052312](https://doi.org/10.1103/PhysRevA.64.052312)
36. K. Wang, J. G. Titchener, S. S. Kruk, L. Xu, H.-P. Chung, M. Parry, I. I. Kravchenko, Y.-H. Chen, A. S. Solntsev, Y. S. Kivshar, D. N. Neshev, A. A. Sukhorukov, Quantum metasurface for multi-photon interference and state reconstruction. [arXiv:1804.03494](https://arxiv.org/abs/1804.03494) (2018).
37. E. Karimi, R. W. Boyd, PHYSICS. Classical entanglement? *Science* **350**, 1172–1173 (2015). [doi:10.1126/science.aad7174](https://doi.org/10.1126/science.aad7174) Medline
38. M. Fiorentino, F. N. C. Wong, Deterministic controlled-NOT gate for single-photon two-qubit quantum logic. *Phys. Rev. Lett.* **93**, 070502 (2004). [doi:10.1103/PhysRevLett.93.070502](https://doi.org/10.1103/PhysRevLett.93.070502) Medline
39. C. V. S. Borges, M. Hor-Meyll, J. A. O. Huguenin, A. Z. Khouri, Bell-like inequality for the spin-orbit separability of a laser beam. *Phys. Rev. A* **82**, 033833 (2010). [doi:10.1103/PhysRevA.82.033833](https://doi.org/10.1103/PhysRevA.82.033833)